GENERAL PHYSICS

I. MOLECULAR BEAMS*

Academic and Research Staff

Prof. J. R. Zacharias
Prof. K. W. Billman
Prof. J. G. King
Prof. C. L. Searle
Dr. K. Fokkens
Dr. S. G. Kukolich
F. J. O'Brien
M. A. Yaffee

Graduate Students

R. Golub
G. L. Guttrich
D. E. Oates
R. S. Stephenson

RESEARCH OBJECTIVES

Our objectives have changed in the last year, partly as a result of the success of the first low-temperature helium beam experiment.

1. RF Spectra, Atomic Clocks, and Null Experiments

It seems unlikely that we shall continue the general study of radio-frequency spectra of atoms and molecules. The development of cesium atomic clocks has proceeded slowly, because of the press of other work, but the techniques already developed, such as high-intensity alkali beam sources and square-wave phase modulation, have been of great use in other experiments. These include the search for permanent electric dipole moment in atoms, for frequency shifts arising from the confinement of atoms between conducting plates, and for small charges carried by atoms.

2. Research with Low-Temperature Atomic Beams

It is now possible to perform many experiments with beams of cold helium and, with some further development, of cold hydrogen. These experiments can be classified as follows.

(i) Studying the scattering of cold He beams by gas, by other beams and from surfaces, both liquid and solid.

(ii) Observing the diffraction of atoms from gratings and apertures.

(iii) Investigating various properties of liquid helium as exhibited by the emitted atoms.

(iv) Using beams of magnetic atoms as microscopic probes of superconductors.

J. R. Zacharias, J. G. King, C. L. Searle

3. Molecular Microscope – Proposed Development

Consider a surface in high vacuum which is emitting neutral molecules. If the molecules moving in the appropriate direction were allowed to pass through a small aperture (pinhole) to strike an array of field-ionization detectors,[1] the resulting ions could be accelerated to a fluorescent screen where a visible image representing the spatial distribution of neutral molecule emission from the surface would be formed.

Improvements in the image would require the development of a suitable atom-light

*This work was supported by the Joint Services Electronics Programs (U.S. Army, U.S. Navy, and U.S. Air Force) under Contract DA 36-039-AMC-03200(E), and in part by the Sloan Fund for Basic Research (M.I.T. Grant 99).

transducer with good resolution and high quantum efficiency and stability. Although the density of field-ionization detectors could be increased, perhaps, by using whiskers or Si fibers instead of needles, a better system might be to adsorb the atoms on a cold surface, where sideways motion is slight, and to read out by simultaneously desorbing and ionizing with a scanning electron beam. The desorbed ions could then strike a fluorescent screen. Methods by which transmitted electrons or generating photons are used directly might also be possible.

Lenses may be used instead of a pinhole to increase the aperture of the system if the molecules have electric or magnetic moments. This is particularly easy when cold beams are used. The effects of the velocity dependence of the focal length can be avoided by chopping the beam and "reading out" the detector at appropriate times. One then also learns about the velocity dependence of the scattering.

Besides observing molecules from desorbing or outgassing surfaces, one could bombard the surface with charged particles and examine the ejected neutrals or expose the surface to beams of neutral molecules and examine the scattered beams. Various properties of the object could be studied by varying both its temperature and that of the incident beam and by using incident molecules with and without electric and magnetic moments. State-selected beams could also be used. It seems likely that one could view a helium surface or a superconductor by emitted or scattered molecules. If the neutral molecule, ion, and light systems can each be made to have a magnification of, say, 100X while preserving adequate resolution, one might be able to observe large molecules; but this is a distant possibility.

Although there are still many unknown problems, and no very elaborate study has yet been undertaken, it seems possible to develop a useful "molecular microscope." Such a device would be a complement to photon, electron, and ion microscopes and might be useful in metallurigical, chemical, and especially biological research.

J. G. King

References

1. W. D. Johnston, Jr. and J. G. King, Rev. Sci. Instr. 37, 475 (1966).

A. SQUARE-WAVE PHASE MODULATION IN MOLECULAR BEAM RESONANCE EXPERIMENTS

The method of square-wave phase modulation was developed by Bates, Badessa, and Searle[1] for use on cesium beam frequency standards. This system offers the advantage over other modulation schemes that very high fidelity modulation, that is, free from distortions and asymmetries, may be easily achieved by modulating the resonant frequency of a tuned rf amplifier. This is especially important in high-precision frequency comparison experiments. This system has the added advantage of providing a convenient method of measuring cavity phase difference, or velocity-dependent shifts arising from $\vec{v} \times \vec{\mathscr{E}}$ in separated oscillating-field resonance experiments.

1. Theory of Sqaure-Wave Phase Modulation

A simplified theory of square-wave phase modulation will be presented elsewhere.[2] In the following discussion there will be no restrictions on frequency or cavity phase deviations, and we shall keep all terms that may have a significant

effect on the shape of the resonance.

The transition probability for a separated oscillating-field resonance apparatus[3] is

$$P = \sin^2\left(\frac{2bl}{v}\right)\cos^2\left[\frac{(\omega_o-\omega)L}{2v}-\frac{\phi}{2}\right],$$

where ω_o is the atomic resonance frequency, L is the cavity separation, v is the velocity of the atoms, l is the RF interaction length, b is the transition rate in the cavities, and ϕ is the cavity phase difference. In an atomic beam apparatus the beam intensity at the detector is proportional to the intergral of P over the velocity distribution.

$$i = i_o + A\int_0^\infty n(v)\sin^2\left(\frac{2bl}{v}\right)\cos\left[\left(\frac{\omega_o-\omega}{v}\right)L-\phi\right]dv.$$

The square-wave modulation steps the phase of the stimulating signal back and forth from approximately +90° to -90°, with a period of approximately four times the average transit time τ_a, the time required for a molecule to travel from the first cavity to the second. The effect of this modulation is to produce an apparent phase difference between the microwave cavities. Immediately after the phase of the stimulating signal is changed, all of the atoms between the cavities will encounter a phase in the second cavity which is different from that in the first cavity. This produces an apparent cavity phase difference, ϕ_1, which persists for the transit time, τ. The cavity phase difference ϕ is composed of two parts, $\phi = \phi_o + \phi_1$, where ϕ_o is a constant (varies at a rate that is slow compared with the modulation) cavity phase difference, and ϕ_1 is the transient, apparent cavity phase difference produced by modulating the phase of the stimulating signal.

$$i(t) = i_o + A\int_0^\infty n(v)\left\{\cos\left[(\omega_o-\omega)\frac{L}{v}-\phi_o\right]\cos\phi_1(t')\right.$$

$$\left.-\sin\left[(\omega_o-\omega)\frac{L}{v}-\phi_o\right]\sin\phi_1(t')\right\}\sin^2\left(\frac{2bl}{v}\right)dv,$$

where $t' = t - \frac{L_1}{v}$, with L_1 the distance from the second cavity to the detector.

The modulation produces steps of $\pm\phi_m$ in the value of ϕ_1, so we may write

$$\cos\phi_1(t) = M(t)\cos\phi_m$$

$$\sin\phi_1(t) = N(t)\sin\phi_m,$$

where M and N may have the values 0, ±1, and the amount of modulation is expressed in ϕ_m. The time dependence of the cavity phase difference ϕ_1, M and N is shown in Fig. I-1. The modulation period is 2T. In an actual resonance experiment the strength

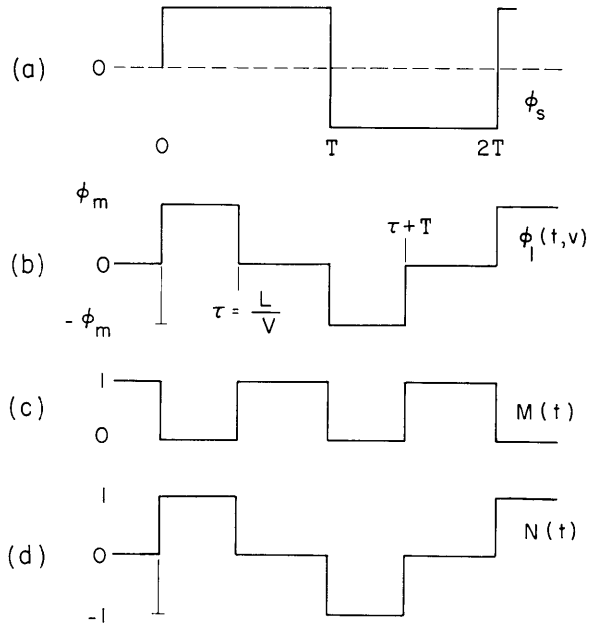

Fig. I-1. Apparent cavity phase difference ϕ_1, M and N as a function of time.

of the rf field is adjusted to give the maximum resonance signal, and this occurs for $2bl/v_a = \tau/2$, where v_a is the average velocity in the beam. Now the expression for the beam intensity is

$$i(t) = i_o + A \cos \phi_m \int_0^\infty n(v) \sin^2\left(\frac{\pi v_a}{2v}\right) \cos\left[(\omega_o-\omega)\frac{L}{v} - \phi_o\right] M\left(t - \frac{L_1}{v}\right) dv$$

$$- A \sin \phi_m \int_0^\infty n(v) \sin^2\left(\frac{\pi v_a}{2v}\right) \sin\left[(\omega_o-\omega)\frac{L}{v} - \phi_o\right] N\left(t - \frac{L_1}{v}\right) dv. \qquad (1)$$

We note that the second term will produce no fundamental component at the modulation frequency $\frac{1}{2T}$, since M has a period, T. The modulation amplitude ϕ_m only comes in through the factor sin ϕ_m, so this will have no effect on the shape of the resonance pattern, and the optimum value is $\phi_m = 90°$.

The effect of a synchronous detector is to perform a Fourier analysis of i(t). Since N(t+T) = -N(t), this is given by

$$\Phi = \frac{\pi}{T} \int_0^T \sin\left(\frac{\pi t}{T} - \phi_1\right) i(t)\, dt,$$

where ϕ_a is the reference phase for the synchronous detector. Since $N\left(t - \frac{L_1}{v}\right)$ is the only nonvanishing factor that is time-dependent, we obtain

$$\Phi(\omega) = A \sin \phi_m \int_0^\infty n(v) \sin\left[(\omega_o - \omega)\frac{L}{v} - \phi_o\right]$$

$$\times \left[\cos\left(\frac{\pi(L_1+L)}{Tv} - \phi_a\right) - \cos\left(\frac{\pi L_1}{Tv} - \phi_a\right)\right] dv. \qquad (2)$$

The optimum modulation frequency, $\frac{1}{2T}$, is approximately $\frac{1}{4\tau_a}$, where L/τ_a is the average velocity in the beam. The optimum value of ϕ_a depends on the length of the region between the second cavity and the detector. The optimum value of ϕ_a for the in-phase synchronous detector is typically 0.2 radian, or less, and is determined experimentally as the phase that gives the maximum amplitude of the resonance signal $\Phi(\omega)$. The quadrature synchronous detector is then operated at a phase of $\phi_a + 90°$ with respect to the modulation.

2. Experimental Results

A cesium beam magnetic resonance apparatus with 125-cm cavity separation was used to test the square-wave phase-modulation system and to obtain values for parameters in the theoretical expression for the resonance function. The cesium hyperfine transition $(4, 0 \rightarrow 3, 0)$ was observed in this apparatus with a linewidth of 140 Hz. The modulation frequency was $\frac{1}{2T}$ = 53 Hz. The distance from the second cavity to the detector was L_1 = 68 cm, and the optimum value of ϕ_a for the in-phase synchronous detector was −0.21 radian.

The experimental resonance pattern was obtained by sweeping the stimulating signal frequency slowly (~2Hz/sec) through the resonance and recording the output of the synchronous detectors on a strip chart recorder. Theoretical resonance patterns calculated on a computer by putting a velocity distribution n(v) with adjustable parameters into (2),

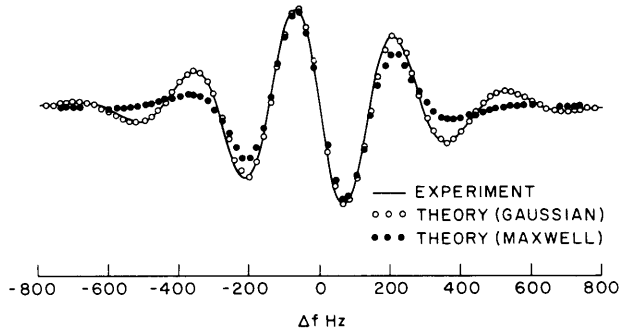

Fig. I-2.
Experimental and theoretical resonance patterns, I(ω), as a function of frequency.

the expression for $\Phi(\omega)$, and adjusting the parameters for a good fit to the experimental pattern. The velocity distributions employed were a modified Maxwellian distribution

$\left(n(v) = n_o v^3 e^{-(v/a)^2}\right)$ and a Gaussian distribution $\left(n(v) = n_o e^{-\beta(v-v_o)^2}\right)$. The experimental and theoretical resonance patterns, $I(\omega)$, are shown in Fig. I-2 $[I(\omega) \equiv \Phi(\omega, \phi_a = -0.21)]$. The Maxwellian distribution contains only one adjustable parameter and when the average velocity is fitted to the data, the resulting Maxwellian velocity distribution is broader than the experimental velocity distribution. This effect is apparent in Fig. I-2. since the width of the envelope of the resonance function is inversely related to the width of the velocity distribution. The Gaussian distribution contains two adjustable parameters and, with the proper values of the parameters v_o and β, provides an accurate fit to the observed resonance pattern. The best fit for the Maxwellian distribution was obtained with $a = 297$ m/sec. The best fit for the Gaussian distribution was obtained with $v_o = 368$ m/sec, $\beta = 6.56 \times 10^{-5}$ $(\text{sec/m})^2$. We believe that the observed velocity distribution is narrower than the Maxwellian distribution because the narrow gap width of the deflecting magnets removes atoms from the beam if their deflection is much greater or much less than the average deflection.

We have determined the velocity distribution by fitting the resonance pattern, and we shall now use this distribution to determine the behavior of the quadrature signal. The Gaussian distribution was used to calculate the quadrature output signal $Q(\omega)[Q(\omega) \equiv \Phi(\omega, \phi_a = 1.78)]$. The experimental and theoretical values of $Q(\omega)$ are shown in Fig. I-3.

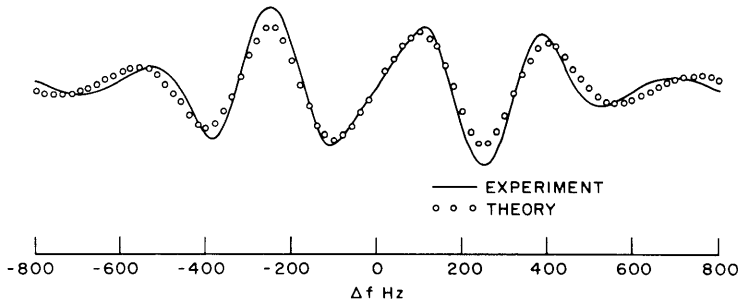

Fig. I-3. Experimental and theoretical values of the quadrature output signal, $Q(\omega)$, as a function of frequency.

In the next experiment the output of the in-phase synchronous detector $I(\omega)$ was used in a servo loop to control the frequency of the stimulating signal. This system maintained the stimulating frequency on the center of the resonance pattern (at $I(\omega) = 0$). Under there conditions, the cavity phase difference, ϕ_o, was varied and the output from the quadrature synchronous detector was measured and calculated as a function of ϕ_o. The results of these measurements and calculations are shown in Fig. I-4. We see that the quadrature signal is linearly related to the cavity phase difference ϕ_o over the range $\phi_o = -60°$ to $+60°$, and that the sensitivity is greater for a wider velocity distribution.

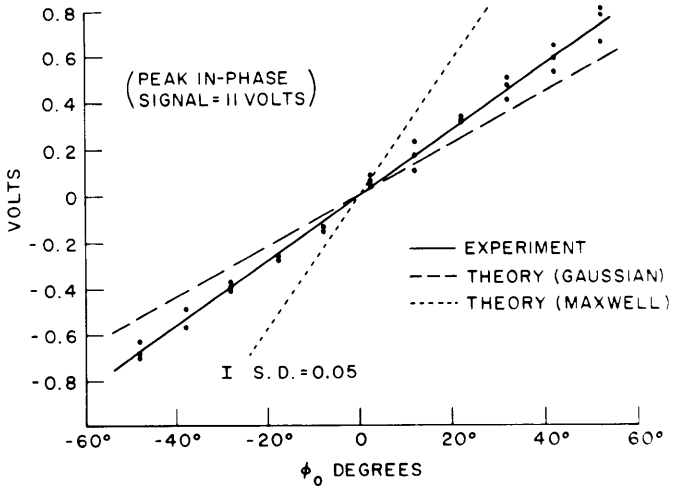

Fig. I-4. Quadrature output signal as a function of cavity phase difference, ϕ_o, with $I(\omega) = 0$.

Therefore, in a two-cavity frequency standard the quadrature signal can be used to control the cavity phase shift.

In experiments in which a large electric field is applied to the region between the cavities, a velocity-dependent frequency shift is produced by the $\vec{v} \times \vec{\mathscr{E}}$ contribution to the magnetic field. In order to show that this system has the same behavior for a velocity-dependent frequency shift such as this $\vec{v} \times \vec{\mathscr{E}}$ term, we note that the transition probability near resonance is approximately

$$P = \frac{1}{2} \cos \left[\left(\omega_o^* - \omega \right) \frac{L}{v} - \phi_o \right]$$

and if

$$\omega_o^* = \omega_o + 2\pi \left(\frac{-\mu_J/h}{8J} \right) \frac{v}{c} \vec{\mathscr{E}}_o \sin \gamma,$$

this is equivalent to using ω_o, ϕ_o^*, where

$$\phi_o^* = \phi_o - 2\pi \left(\frac{-\mu_J/h}{8J} \right) \frac{L}{c} \vec{\mathscr{E}}_o \sin \gamma,$$

so we see that the $\vec{v} \times \vec{\mathscr{E}}$ frequency shift has the same effect on the transition probability as a cavity phase difference of $\left(\phi_o^* - \phi_o \right)$. We note that the $\vec{v} \times \vec{\mathscr{E}}$ shift is only present when a large electric field is applied to the region between the cavities, so we may measure ϕ_o independently by turning off the electric field.

Finally, a more direct experimental check on the velocity spectrum can be made, because, on the center of the resonance, the time derivative of the beam current is

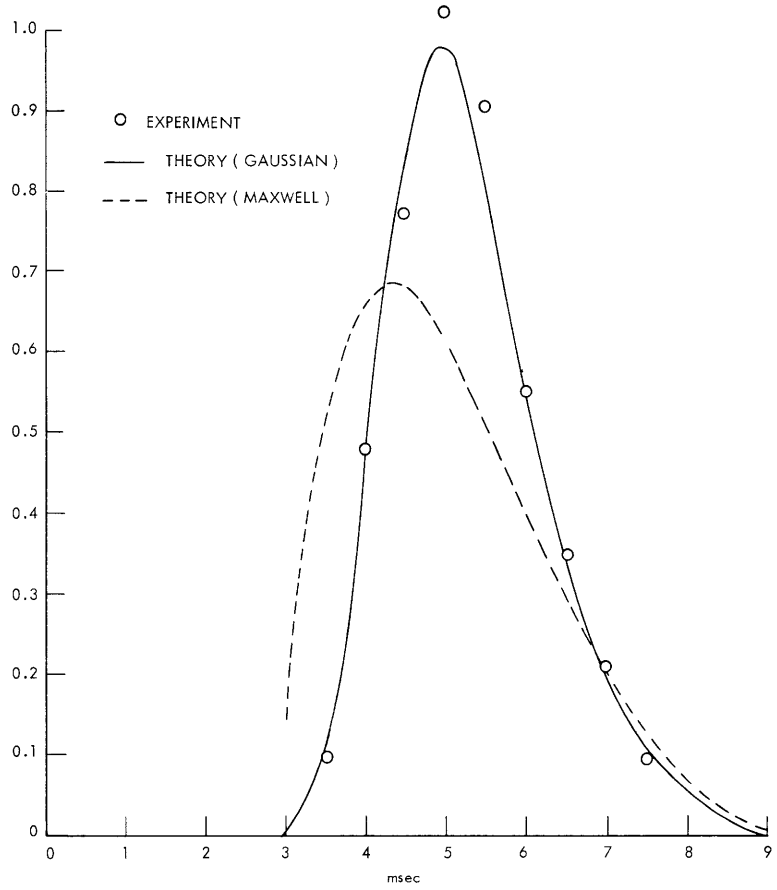

Fig. I-5. Modified distribution of transit times.

related to the velocity distribution in a simple way. For the conditions $\omega_o = \omega$, $\phi = 0$ and $0 < t < T$ we see from Eq. 1 that

$$\frac{di(t)}{dt} = A \cos \phi_m \, n\left(\frac{L+L_1}{t}\right) \sin^2\left(\frac{\pi v_a t}{2(L+L_1)}\right),$$

where n(v) is the velocity distribution, and t is the time measured from the last modulation step. This is just the distribution of transit times from the first cavity to the detector multiplied by the average of a $\sin^2$ factor. The $\sin^2$ term has the effect of making the distribution of transit times appear narrower. The second maximum occurs at times so great that $n\left(\frac{L+L_1}{t}\right)$ is nearly zero. The experimental and theoretical results for this function are shown in Fig. I-5. The experimental data were obtained by averaging over many cycles of the modulation with a multichannel analyzer. The channel number was proportional to time t, and the number of channel counts was proportional to the beam current i(t).

S. G. Kukolich, K. W. Billman

References

1. R. S. Badessa, V. J. Bates and C. L. Searle, IEEE Trans., Vol. IM-13, p. 175, 1964.
2. S. G. Kukolich and K. W. Billman (to appear in J. Appl. Phys.).
3. N. F. Ramsey, Molecular Beams (Oxford University Press, London, 1956), Chap. 5.
4. S. G. Kukolich, Proc. IEEE 52, 211 (1964).

B. SEARCH FOR A SHIFT IN THE TRANSVERSE ELECTROMAGNETIC MASS OF THE ELECTRON

Power has suggested[1] that a shift in the frequency of an atomic clock can be produced by confining the atoms passing through the transition region between conducting plates. The mechanism of this shift can be described as follows: Part of the experimental mass of an electron is due to the presence of a cloud of virtual photons surrounding the "bare" electron. If one should place the electron between conducting walls, virtual photons of a wavelength greater than L, the wall separation, could no longer exist. Hence, the confinement produces a mass shift. A cesium clock utilizes a hyperfine transition involving the reorientation of a single 6s electron outside a closed shell. The frequency of this transition is proportional to the square of the mass of this electron. Hence one might expect $\Delta\nu/\nu = 2\Delta m/m$. Power's calculation gives an estimate of

$$\frac{\Delta\nu}{\nu} \approx 4\alpha\frac{\lambda_c}{L} = \frac{7.1 \times 10^{-11}\ \text{mm}}{L},$$

where α is the fine-structure constant, λ_c is the Compton wavelength of the electron, and L is the separation between the conducting plates.

A search for such a shift was made by using a Cs atomic clock of the usual separated cavity type[2] modified to include movable plates in the "C" region between the RF cavities. Provision for external adjustment of the plate gap ($L = 0.4$ mm to $L = L_o \approx 25$ mm) necessitated the removal of the usual magnetic shielding of this region which led to some drift uncommon to a high-stability clock; however, as will be explained later, this was easily monitored. A second Cs clock was used as a frequency standard, thereby allowing for simple comparisons to be made to determine any changes in the "experimental clock" frequency as its plates were set to various gaps.

The experimental clock C region between cavities was 126 cm. The linewidth of the resonance at the $(F = 4, m_F = 0) \longrightarrow (F = 3, m_F = 0)$ hyperfine transition frequency of 9192 MHz was 140 Hz. The movable, conducting plates, 2.54 cm high and 71 cm long, were made of gold-plated aluminum. Gap adjustment was effected by means of manipulators, one of which was connected to each end of each plate. These allowed for a

simple alignment of the plate axis along the beam axis by observing a sudden decrease in "flop" signal as the gap was narrowed. To obviate direct contact of the beam with the plates, four beam stops were used to limit the beamwidth. Subsequently, the plate gap was never allowed to become smaller than this width, which was 0.4 mm. It should be noted that when the beam was allowed to impinge on the plates, unreproducible frequency shifts were observed which, although interesting, could not be profitably investigated with the present apparatus.

An excellent running check on the sensitivity of the apparatus was obtained by placing a potential difference across the normally grounded plate and observing the Stark shift. This also allowed a simple measurement of the gap size.

Measurements were performed under two different magnetic field configurations in the C region. In Case 1, the magnetic field has a major component vertical, that is, parallel to the conducting plates, of approximately 0.5 Gauss. In Case 2, the major component was perpendicular to the plates and of approximately 0.1-Gauss magnitude. On this basis, it is easy to see that the Case 2 data are expected to be more reliable than those of Case 1, since for the (4, 0) → (3, 0) hyperfine transition $\delta f = 427\ B^2\ \frac{Hz}{Gauss^2}$, where δf is the second-order magnetic field frequency for the shift B. Thus if the field varies by a small amount ΔB, a shift $\Delta(\delta f) = 854\ B\Delta B\ \frac{Hz}{Gauss^2}$ results. In the Case 1 experiment a 2-milligauss field variation produces a shift of $\Delta\nu = 0.854$ Hz, or $\frac{\Delta\nu}{\nu} \approx 9 \times 10^{-11}$, which was about the largest excursion seen during the experiment. In the Case 2 experiment, however, the same field variation would produce a fivefold smaller shift. One would then expect smaller fluctuations, as was found, and less systematic error with this method of operation.

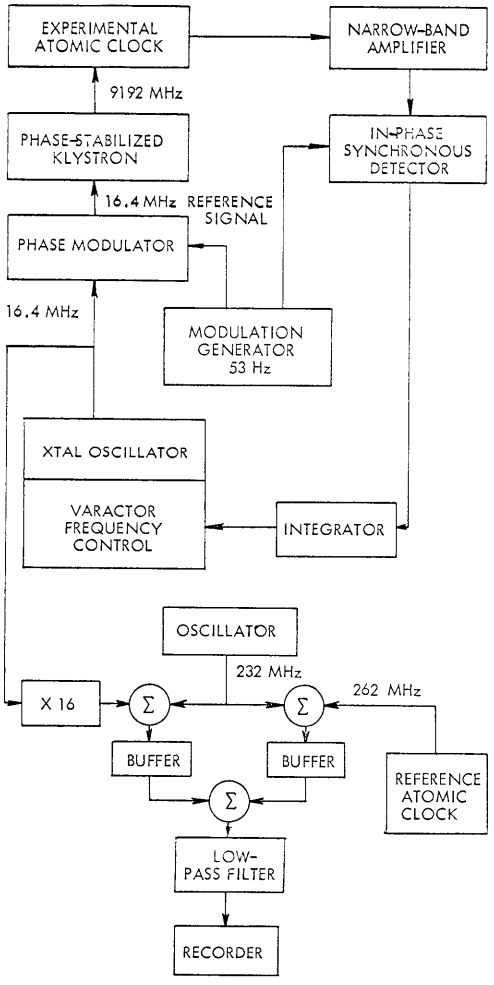

Fig. I-6. Schematic of the electronics.

Data were gathered with the plates alternately wide ($L = L_o = 25$ mm) and narrow. This allowed the effects of drifts to be eliminated to first order. This

correction was generally not necessary for Case 2 data.

Figure I-6 illustrates schematically the electronic apparatus used for the measurement. The reference clock, which utilized a National NC-2001 beam tube, has a measured stability of 3×10^{-12} for a 10^3-sec averaging time. Heterodyning the 262-MHz signals obtained from each clock with a local oscillator allowed a simple display of the beat. Frequency-shift measurements were then made by examination of the beat frequency as the plate gap in the experimental clock was varied.

The experimental results are displayed in Fig. I-7. Each point represents approximately 500 seconds of data with the plates at L_o, and 500 seconds at L. The dashed

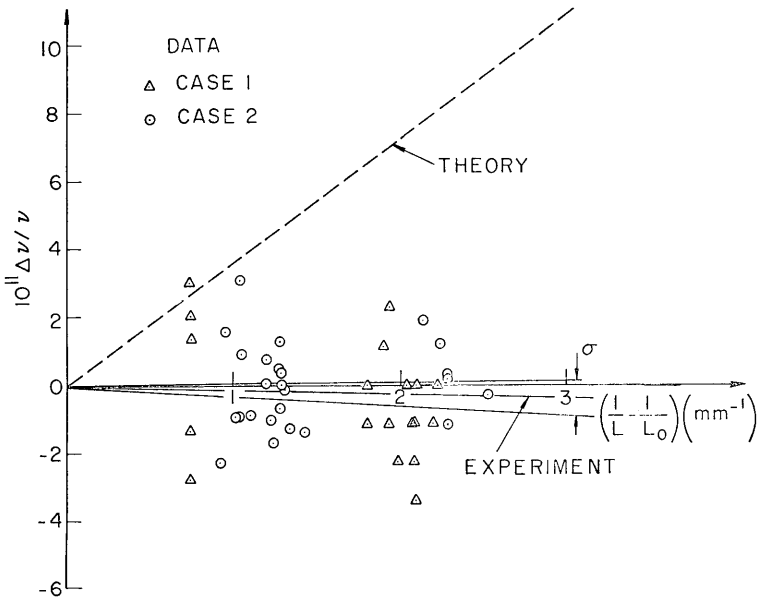

Fig. I-7. Experimental data.

line indicates a frequency shift that would be expected if $\Delta\nu/\nu = (0.56)\, 4a\frac{\lambda_c}{L}$, where the numerical factor of 0.56 arises from the fact that the plates only "filled" the C region to this extent. The slope of this line is 4×10^{-11} mm. A least-square fit of the Case 1 data gives a line of slope $\langle a \rangle_1 = (-2.5 \pm 2.5) \times 10^{-12}$, 19 measurements, whereas the slope of the Case 2 data gives $\langle a \rangle_2 = (-0.14 \pm 1.73) \times 10^{-12}$, 25 measurements. Since there is no obvious reason to believe that the field direction affects the predicted hyperfine splitting, these measurements may be combined by using standard weighting with the inverse square of the respective standard deviations, to give $\langle a \rangle_{1+2} = (-0.9 \pm 1.4) \times 10^{-12}$, 44 measurements.

G. L. Guttrich, K. W. Billman

References

1. E. A. Power, Proc. Roy. Soc. (London) A292, 424 (1966).
2. N. F. Ramsey, Molecular Beams (London: Oxford University Press, 1956).